

Dynamical transport of asteroid fragments from the ν_6 resonance

Takashi Ito^a and Renu Malhotra^b

^a*Center for Computational Astrophysics, National Astronomical Observatory of Japan, Osawa 2-21-1, Mitaka, Tokyo 181-8588, Japan.*

^b*Lunar & Planetary Laboratory, University of Arizona, 1629 E. University Boulevard, Tucson, AZ 85721-0092, USA*

Abstract

A large disruption in the main asteroid belt can cause a large flux, an “asteroid shower”, on the terrestrial planets. We quantitatively examine the hypothesis that such an event was the cause of the lunar late heavy bombardment (LHB). We performed numerical integrations of about 20000 test particles starting in the vicinity of the ν_6 secular resonance in the main asteroid belt. The purpose of these integrations is to calculate, for each of the terrestrial planets, the collision probability of asteroids coming from an asteroid break-up event in the inner part of the main belt. Compared with previous studies, we simulate nearly two orders of magnitude larger number of particles, and we include the orbital effects of the eight planets, Mercury to Neptune. We also examined in detail the orbital evolution of asteroid fragments once they enter the Earth’s activity sphere, including the effect of the Earth–Moon orbit. We obtained the collision probability, the distributions of impact velocities, impact positions, and impact angles of asteroid fragments on the Moon. The collision probability with the Moon ($\sim 0.1\%$) suggests that a fairly large parent body, 1000–1500 km in diameter, is required if the LHB event is to be ascribed to a single asteroid disruption. An even larger parent body is required for less favorable initial conditions than we investigated here. We conclude that an asteroid disruption event is not a viable explanation for the LHB.

Key words: Asteroid, celestial mechanics, resonance, collision, crater

Email address: ito.t@nao.ac.jp (Takashi Ito).

1 Introduction

Among the many aspects of the impact history of the terrestrial planets related to asteroids, the crater record on the Moon and the intense collisional event collectively called the late heavy bombardment (LHB) or the terminal lunar cataclysm around 4 Ga (cf. Ryder, 1990; Hartmann et al., 2000) is particularly interesting. Evidence of LHB began to accumulate when Ar–Ar isotopic analyses of Apollo and Luna samples suggested several impact basins of the nearside of the Moon had been produced during the 3.88–4.05 Ga interval (Tera et al., 1973, 1974). Recent results on the impact ages of lunar meteorites also suggest that an intense period of bombardment on the Moon occurred about 3.9 Ga, i.e. 0.5–0.6 billion years after the formation of the Earth–Moon system (Cohen et al., 2000; Kring and Cohen, 2002).

The discussion on the existence or non-existence of the lunar cataclysm is still somewhat controversial. Meanwhile the search for the possible dynamical cause of LHB is as important as the geological and geochemical research of the event itself. At present, there is no good consensus on the nature or the source(s) of the impactors. Recent papers have suggested that LHB may have been due to a large flux of asteroids and comets (Kuiper Belt objects) in the inner solar system caused by the orbital migration of the outer planets (Levison et al., 2001; Gomes et al., 2005). Another possible cause of the LHB that has been suggested previously — and one that we examine in the present work — is a temporary and heavy asteroid shower created by a large collisional event in the main asteroid belt (Zappalà et al., 1998). Zappalà et al. (1998) evaluated the number of impactors produced in different size ranges by disruption events that might have created some of the existing asteroid families. Their estimates show that an impact flux from such an asteroid-disruption event, lasting 2–30 million years in the form of asteroid showers, could be responsible for the lunar cataclysm.

Previous studies, including Zappalà et al. (1998), Gladman et al. (1997) and Morbidelli and Gladman (1998), have estimated the collision probability of asteroid fragments and the timescale of its flux on the terrestrial planets. However, all these studies have been obliged to use somewhat simplified dynamical models, and were limited to simulations with a relatively small number of particles (a few hundreds to a few thousands), mainly because of computer resource limitations. Also, no previous study has included the orbital dynamics of the Earth–Moon system when estimating the collisional probability of the asteroid fragments on the Earth or on the Moon. Because the typical collision probabilities with the planets are a few percent or less, previous simulations have typically yielded only a few colliders, and consequently their quantitative estimates of collisional probabilities have significant uncertainties. As we move closer towards the goal of accurately calculating the collision frequency

and probability of asteroid fragments on terrestrial planets, we would like to improve the statistics by simulating much larger numbers of particles and also assessing the effects of the modeling simplifications in previous studies.

The purpose of this paper is to provide a better statistical result on the collision probability of asteroid fragments with the terrestrial planets. We consider asteroid fragments coming from low inclination orbits at the ν_6 secular resonance in the main asteroid belt. We choose this resonance because it is presently one of the strongest resonances for the transport of asteroids and meteorites to the inner solar system. For our study, we numerically analyze the orbital evolution of more than 20000 test particles, with initial conditions that simulate hypothetical asteroid disruption events in the vicinity of the ν_6 . We also performed an additional set of orbital simulations of a large number of test particles as they evolve within the Earth's activity sphere, including the dynamical effects of the Earth-Moon orbit. (The initial conditions for the latter simulations are derived from the orbital distribution function of those particles originating from the vicinity of the ν_6 that manage to enter the Earth's activity sphere.) For the range of initial source locations that we consider in this study (low inclination orbits near the ν_6), our results provide the best estimates currently available for asteroid collision probabilities on each of the terrestrial planets, as well as for the distributions of impact velocity, impact angle and spatial distribution of impacts on the Moon.

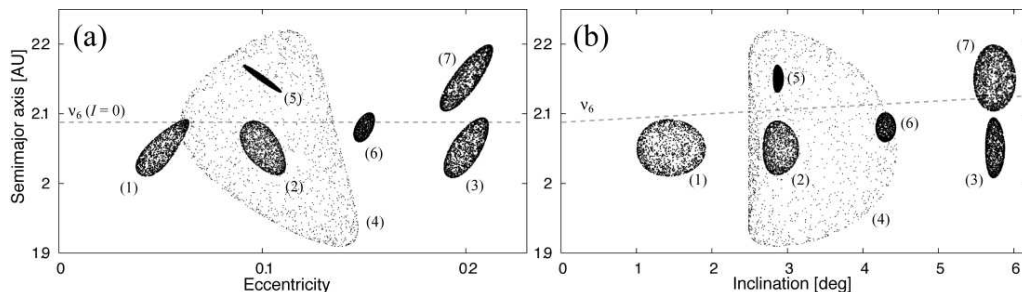


Fig. 1. Initial osculating orbital elements of the asteroid fragments in our numerical integrations. (a) Eccentricity e and semimajor axis a . (b) Inclination I and semimajor axis a . The dashed lines in each panel indicate the approximate location of the ν_6 resonance (Morbidelli and Henrard, 1991).

2 Dynamical model and initial conditions

We start with test particles near/in the ν_6 resonance and numerically integrate their orbital evolution under the gravitational effect of eight major planets, from Mercury to Neptune. The major planets are assumed to have their present masses and orbital elements. All celestial bodies are treated as point masses dynamically, although planetary and solar physical radii matter when we calculate collisions between a test particle (i.e. an asteroid fragment) and a large body. No consideration is given to post-Newtonian gravity, tidal force, gas drag, solar equatorial bulge, and other non-gravitational or dissipative effects such as the Yarkovsky effect.

To emulate disruption events that create a swarm of asteroid fragments, we assume isotropic and equal-velocity disruptions; all fragments have the same and isotropic initial ejection velocity, v_0 . We chose $v_0 = 0.1$ or 0.2 km/s, and we also tested $v_0 = 0.8$ km/s for comparison. We selected seven initial positions of asteroid fragments to sample a range of locations in the vicinity of ν_6 in orbital element space (a, e, I) as in Fig. 1. The detailed initial conditions are shown in the upper part of Table 1. We created sets of orbital elements of asteroid fragments as follows: (1) Select an appropriate point in the osculating orbital element space as a disruption center. This fixes six orbital elements of the disruption center; equivalently, six variables of three dimensional position and velocity of the disruption center $(\mathbf{r}, \mathbf{v}) = (x, y, z, v_x, v_y, v_z)$ in Cartesian coordinate. (2) Give an ejection velocity, \mathbf{v}_0 , as in Table 1 to each of the hypothetical asteroid fragments so that a fragment’s velocity becomes $\mathbf{v} + \mathbf{v}_0$ in Cartesian coordinates. For each fragment, we add \mathbf{v}_0 with the same magnitude $|\mathbf{v}_0|$ with different directions using random numbers so that the disruption becomes “isotropic”. (3) Finally, convert the coordinates and velocities of the fragments, $(\mathbf{r}, \mathbf{v} + \mathbf{v}_0)$, into six osculating orbital elements; the resulting a, e, I distributions are shown in Fig. 1.

For the currently existing asteroid families, estimates of the initial ejection velocity of asteroid fragments are in the range of $v_0 = 0.1$ – 0.2 km/s (Zappalà et al., 1996; Cellino et al., 1999). However, this is an overestimate, because account must be taken of the Yarkovsky thermal force which works effectively on asteroid families to increase their velocity dispersion over time (Farinella et al., 1998; Bottke et al., 2001). Thus, our adopted values of v_0 , are actually somewhat larger than those of the disruptions that created the observed asteroid families, but are appropriate for the putative breakup of a parent body as large as 1000–1500 km in diameter, which, as we show later, would be necessary to cause the LHB in this scenario.

For each of the seven initial disruption locations, we placed about 3000 test particles (20756 particles in total), and numerically integrated their orbital

evolution for up to 100 million years. When a test particle goes within the physical radius of the Sun or that of planets, we consider the particle to have collided with that body, and remove it from the computation. Also, when the heliocentric distance of a test particle gets larger than 100 AU, the particle’s integration is stopped. The “survivors” are particles that remain within 100 AU heliocentric distance without colliding with the Sun or any planet for 100 Myr. For the numerical integration we used the regularized mixed-variable symplectic method (SWIFT_RMVS3 by Levison and Duncan (1994)).

We should explain here the reasons why we have selected initial conditions that are very close to the ν_6 resonance. We do not necessarily think that these are realistic initial conditions of actual asteroid disruptions in the main belt. Large asteroids are not likely to remain close to a strong resonance, such as the ν_6 , for hundreds of million years (which is the time interval between the planet formation era and the LHB). Thus, large collisional disruptions, if they occur, would be expected to be centered away from strong resonances. However, the fragments that eventually collide with the inner planets are delivered into planet crossing orbits by entering strongly unstable resonance zones. In this manuscript our focus is on obtaining the collision probability of asteroid fragments that are delivered to the inner solar system via the ν_6 . We use as many test particles as computationally feasible in order to obtain the basic orbital statistics data for relevant research. In this sense, we think our choice of initial conditions of test particles close/in the ν_6 resonance is justified and useful for our purpose.

3 Asteroid flux on terrestrial planets

The lower part of Table 1 summarizes the collision probability of test particles on the planets and on the Sun, for each of the simulations. Except for the cases (4) and (5), approximately 70% of the particles collided with the Sun. About 10–15% of the particles were removed by going further away than 100 AU. In our numerical model, the typical dynamical behavior of particles coming from the ν_6 that eventually hit the terrestrial planets and the Sun as well as those particles that are ejected from the system due to scattering by Jupiter, is qualitatively the same as has been demonstrated by previous numerical studies as Gladman et al. (1997) or Morbidelli and Gladman (1998). Because our numerical integrations are focused on the ν_6 with many more particles than the previous studies, and also because we include Mercury in our numerical model, we could observe collisions with Mercury and Saturn (see Table 1), whereas Gladman et al. (1997) did not observe any collisions on these two planets. This is one illustration of the improved collision statistics that our calculations provide.

Case	(1)	(2)	(3)	(4)	(5)	(6)	(7)
N_{tp}	2961	2962	2961	2967	2967	2962	2976
a (AU)	2.05	2.05	2.05	2.05	2.15	2.08	2.15
e	0.05	0.10	0.20	0.10	0.10	0.15	0.20
I (deg)	1.43	2.87	5.73	2.87	2.87	4.30	5.73
ω (deg)	330.1	181.3	206.5	311.3	81.3	35.9	351.2
Ω (deg)	149.8	103.7	192.7	114.7	121.0	103.7	235.8
l (deg)	55.5	102.6	56.0	97.9	205.4	66.5	46.5
v_0 (km/s)	0.2	0.2	0.2	0.8	0.1	0.1	0.2
Sun (%)	66.0	71.6	73.1	47.3	52.8	75.4	65.5
Mercury (%)	1.01	0.68	1.38	0.57	0.37	0.84	0.97
Venus (%)	6.11	5.06	4.56	3.24	2.90	5.00	3.83
Earth (%)	4.42	3.17	2.57	2.90	2.33	3.24	2.96
Mars (%)	0.71	0.64	0.54	0.88	0.94	0.20	0.94
Jupiter (%)	0.91	0.57	0.27	0.61	0.30	0.61	0.94
Saturn (%)	0.03	0.03	0	0	0.03	0.07	0
> 100AU (%)	14.1	13.0	11.6	9.30	10.8	12.7	15.8
survivors (%)	5.44	4.02	4.66	34.1	28.4	0.71	8.27

Table 1

The number of test particles N_{tp} , osculating orbital elements ($a, e, I, \omega, \Omega, l$) of each disruption center, ejection velocity v_0 , and the collision probability of asteroids that hit the Sun and planets in our numerical integrations. The fraction of particles that went beyond 100 AU and that of the particles that have survived over 100 million years are also shown. No collisions with Neptune or Uranus were observed in our simulations.

As shown in Table 1, several per cent of asteroid fragments eventually hit the planets, mostly the terrestrial planets. As described in the next section, the average collision velocity of the fragments with Earth is about 15–20 km/s. Rough average collision velocities with the other terrestrial planets are about 14 km/s for Mars, about 19 km/s for Venus, and about 32 km/s for Mercury. Fig. 2 shows examples of the collision flux with time. Although some of the panels in Fig. 2 have small number statistics, some systematic trends are noticeable. The peak of collision flux on the planets occurs first at Mars, and progressively later at Earth, Venus and Mercury. (This trend is most noticeable in the middle panels, for the case (5) in Fig. 2.) The peak of the collisions with the Sun, as well as the peak of the flux of particles that go too far away (> 100 AU), occurs even earlier than the peak of the collisions with the terrestrial

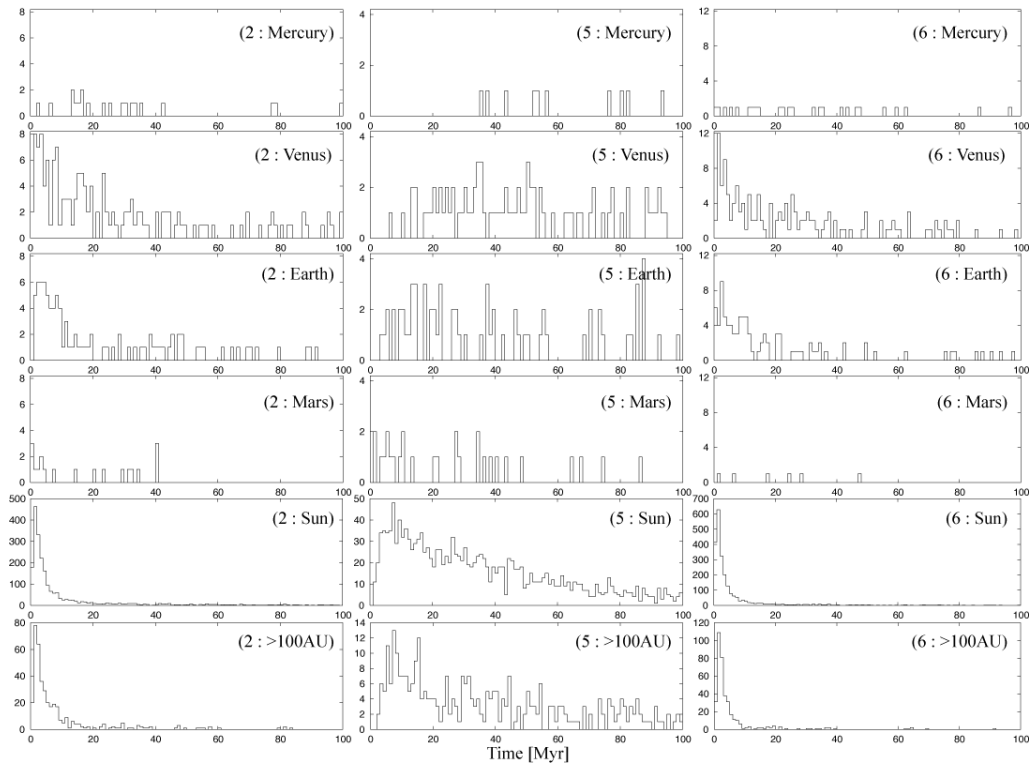


Fig. 2. The number of particles that collided with the terrestrial planets and the Sun, and that went beyond 100 AU starting from the initial conditions (2; left panels), (5; middle panels) and (6; right panels).

planets. Generally in our calculation, e and I of the particles that are close to the ν_6 center are pumped up quickly by ν_6 itself and by an associated Kozai oscillation, in less than a few to ten million years (cf. Michel and Thomas, 1996; Gladman et al., 2000). Many of the particles whose eccentricities reach very high values either directly hit the Sun, or have a close encounter with Jupiter; in the latter case, they are usually scattered outward and are eventually eliminated from the system. This explains both the rapid production and the rapid decay rate of the solar colliders and “too-far” particles. On the other hand, the particles excited to only moderate eccentricity evolve by means of many close encounters with the terrestrial planets which gradually reduce their semimajor axes, making them migrate within the terrestrial planetary

zone on a longer timescale. These particles are the most common candidates for planetary collisions.

The timescale of asteroid flux on the planets strongly depends on the initial location of the fragments and on their initial ejection velocity (Gladman et al., 1997; Morbidelli and Gladman, 1998; Morbidelli and Nesvorný, 1999). When the initial distribution of asteroid fragments is not so widely scattered (i.e. when their v_0 is small) but the location of the disruption event is far away from the resonance center, such as case (5), it takes several million years for particles to achieve planet-crossing orbits, and the flux of solar colliders, too-far particles, and planetary colliders lasts for many tens of millions of years (the middle panels of Fig. 2). This is somewhat in contrast with the cases of those initial conditions whose center is closer to the ν_6 (e.g., cases (2) and (6), Fig. 2): In these cases the flux of solar colliders and too-far particles decays rapidly, with a timescale of 10 million years, although the flux of planetary colliders lasts for many tens of millions of years. We see many survivors in the cases (4) and (5) at 100 myr (Table 1). In contrast, when v_0 of asteroid fragments is small and the location of disruption event is near the resonance center, such as the case (6), the removal efficiency of asteroid fragments is very high, and the impact flux decay timescale is very short as we see in the right panels of Fig. 2.

Table 1 shows that the collision probability of asteroid fragments on Earth is about 3%. Note that we have assumed relatively low initial inclinations for the asteroid fragments; the collisional probability would be lower for higher initial inclinations (cf. Morbidelli and Gladman, 1998). The integrated collision probability for Venus over 100 myr is 1.2–1.7 times larger than that for the Earth. Also, the collision probability for Mercury is somewhat larger than that for Mars (except perhaps in cases (4) and (5) where more planetary collisions would have taken place if we continued the integrations). We can interpret this trend as the combined effect of planetary physical cross sections and average relative velocity of asteroid fragments at each of the planetary orbits, assuming the particle-in-a-box approximation stands. But we need simulations with larger numbers of particles to get more reliable statistics for the differences in collision rates amongst the terrestrial planets. Previous research has used even fewer number of particles in this kind of numerical simulation: For example, Gladman et al. (1997) used only 150 particles for the experiment of the ν_6 resonance, and the number of particles that Morbidelli and Gladman (1998) used was about 400 at ν_6 .

4 Collisions with Earth and Moon

To obtain the collision probability of asteroid fragments with the Moon and to compare it with the lunar crater record, we need to calculate the actual impact flux on the lunar surface. However, looking at our current numerical result described in Fig. 2, the number of planetary collisions is relatively small. For example, starting with a swarm of 3,000 particles, we have about a hundred collisions on Earth over 100 myr. Moreover, the collision probability of asteroid fragments on the Moon in our numerical model would be much smaller than that on the Earth due to the smaller lunar gravity and physical radius, yielding only a few collisions over 100 myr. This poor yield of planetary colliders is the source of the relatively poor statistics from such dynamical models.

However there is a method to improve the collisional statistics for the Moon: although we get only a few hundred planetary colliders in our simulations, we have many more encounters at the planetary activity sphere. The activity sphere, also known as “sphere of influence” (cf. Danby, 1992), of the Earth r_I , which is proportional to $(m_{\oplus}/M_{\odot})^{2/5}$ where m_{\oplus} is the Earth mass and M_{\odot} is the solar mass, is about 144 Earth radii. In our numerical result, about a million encounters took place at this distance in each of the simulated cases. This number is large enough to establish a time-dependent orbital distribution function such as $F(a, e, I, \omega, \Omega, l; t)$ to create “clones” of asteroid fragments in order to increase the reliability of the collision statistics on the Earth–Moon system. What we actually did to generate clones is to slightly change the encounter position \mathbf{r} and velocity \mathbf{v} of each of the original asteroid fragments so that their orbital motion in the activity sphere is a bit different, as $\mathbf{r}_{\text{clone}} = (1 + \delta_r)\mathbf{r}_{\text{original}}$ and $\mathbf{v}_{\text{clone}} = (1 + \delta_v)\mathbf{v}_{\text{original}}$ where $|\delta_r|, |\delta_v| < 0.1$ in our model. Repetition of this procedure produces a large number of clones that obey nearly the same orbital distribution function F as the original particles but with slightly different paths toward the Earth and the Moon. In Fig. 3, we show an example of the integrated distribution of encounter position and velocity of original particles at Earth’s activity sphere that we used to create clones.

We repeated this cloning procedure 1,000 times for each set of integrations that originally involves about 3,000 particles and about a million encounters at r_I . For each of the initial condition sets, the cloning procedure generates three million clones with a billion encounters around Earth’s activity sphere. Using these cloned particles, we performed another set of numerical integrations with the Sun, the Earth, the Moon, and cloned test particles within the Earth’s activity sphere. Here we do not include the effect of other planets, but we do include Moon’s gravity. All the clones start from just outside of Earth’s activity sphere, and all of them go through the sphere until they hit the Earth or the Moon or go out of the sphere. We used the present orbital elements of the Moon, with the true anomaly randomly chosen from 0 to 2π . As for the

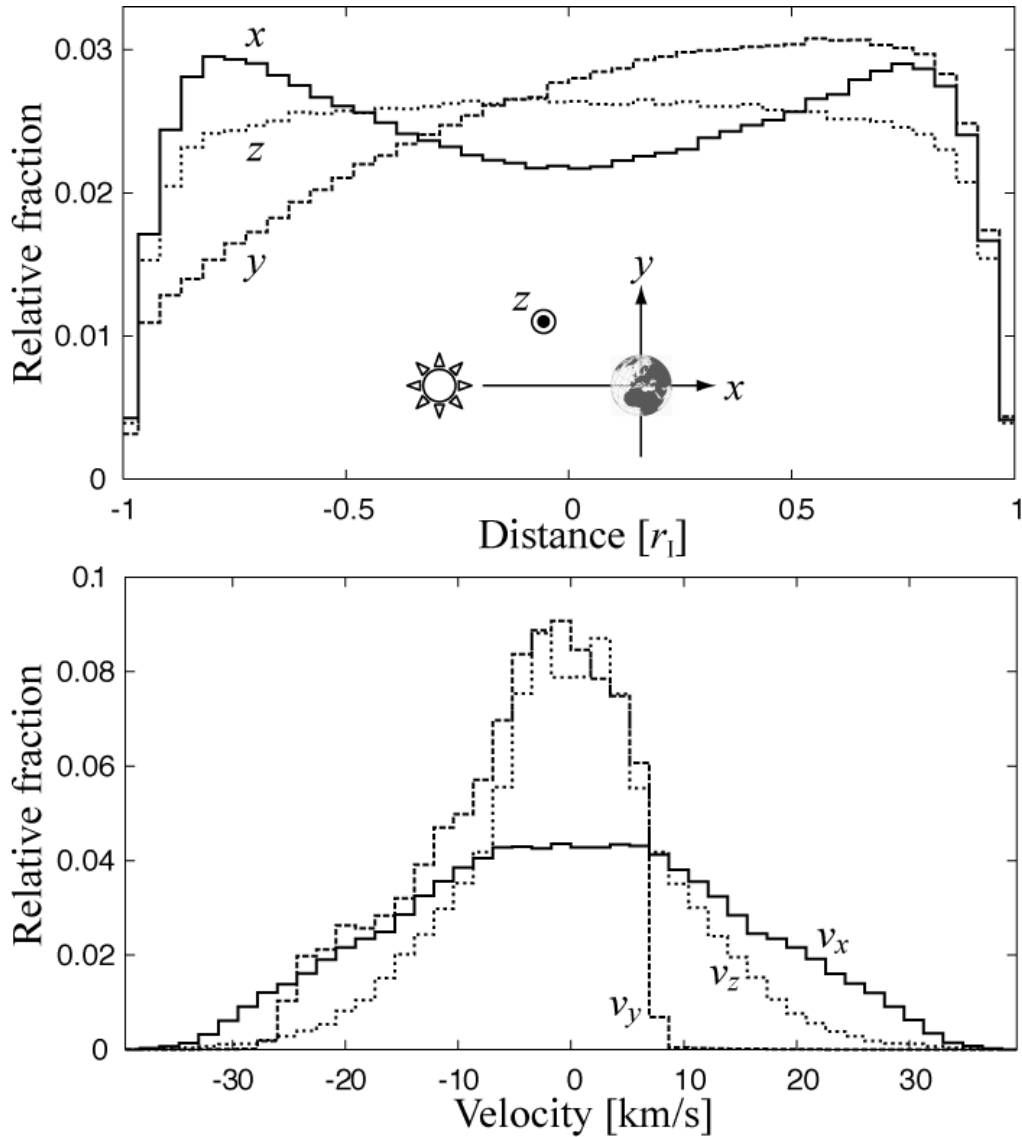


Fig. 3. An example of the statistics at the Earth's r_1 from the case (2). Upper: encounter position of asteroid fragments. Lower: encounter velocity. The coordinates x, y, z are centered on the Earth; x -axis is oriented from the Sun toward the Earth, y -axis is oriented toward the direction that the Earth goes, and z -axis is normal to the Earth's orbit and the north is defined as positive (see the schematic illustration in the upper panel). All statistics are integrated over 100 myr.

numerical method, we use the regularized mixed-variable symplectic method again with a stepsize of 168.75 seconds ($= 2^{-9}$ days). We use geocentric frame for this calculation.

	N_{tp}	N_{enc}	$n_{\text{c,E}}$	$n_{\text{c,M}}$	$P_{\text{c,M}}$	$\frac{n_{\text{c,E}}}{n_{\text{c,M}}}$
(1)	2961	1142636	87486	3708	0.125%	23.6
(2)	2962	1176793	101766	4160	0.140%	24.5
(3)	2961	982652	81359	3618	0.122%	22.5
(4)	2967	777056	72613	2801	0.094%	25.6
(5)	2967	648519	53647	2388	0.080%	22.5
(6)	2962	998867	82014	3501	0.182%	23.4
(7)	2976	758500	66163	2840	0.095%	23.3

Table 2

Collisions of clones on the Moon. N_{tp} is the number of original particles that is also shown in Table 1. N_{enc} is the number of encounters of the original particles with Earth’s activity sphere, r_{I} . These numbers are multiplied by 1,000 to generate clones. $n_{\text{c,E}}$ and $n_{\text{c,M}}$ are the numbers of collisions of clones with the Earth and with the Moon. $P_{\text{c,M}}$ is the collision probability of clones to the Moon ($P_{\text{c,M}}/100 \equiv n_{\text{c,M}}/1000N_{\text{tp}}$).

The resulting collision statistics is summarized in Table 2. Now we have about 10^5 collisions on the Earth ($n_{\text{c,E}}$) and a few thousand on the Moon ($n_{\text{c,M}}$). Overall collision probability of the asteroid fragments on the Moon ($P_{\text{c,M}}$) is about 0.1%, and the number ratio between the collisions on the Earth and on the Moon ($n_{\text{c,E}}/n_{\text{c,M}}$) is about 22–24, which is similar to an analytical estimate (Zahnle and Sleep, 1997).

Not surprisingly, the time-evolution of the impact flux of clones strongly depends on the initial location of asteroid fragments (Fig. 4). Different initial conditions produce a variety of impact decay rates. However, the time-integrated statistics of the impact velocity, the impact angles, and spatial distribution of impacts on the Earth or the Moon are very similar for all initial condition sets; we show the results for one initial condition set (case 2) in Fig 5. This result indicates that the time-integrated characteristics of the impacts on Earth or Moon are not strongly sensitive to the initial velocity dispersion of the asteroid fragments or their distance from the resonance. However, we cannot rule out a dependence of these distributions on initial inclination, since all our initial condition sets had similar low inclinations.

The variety of impact decay rates and the distribution of impact velocity and angles obtained here can be used in future work to create a synthetic crater record of the Moon to compare with the actual lunar craters. We have also calculated the spatial distribution of the impacts on the lunar surface. (Note the

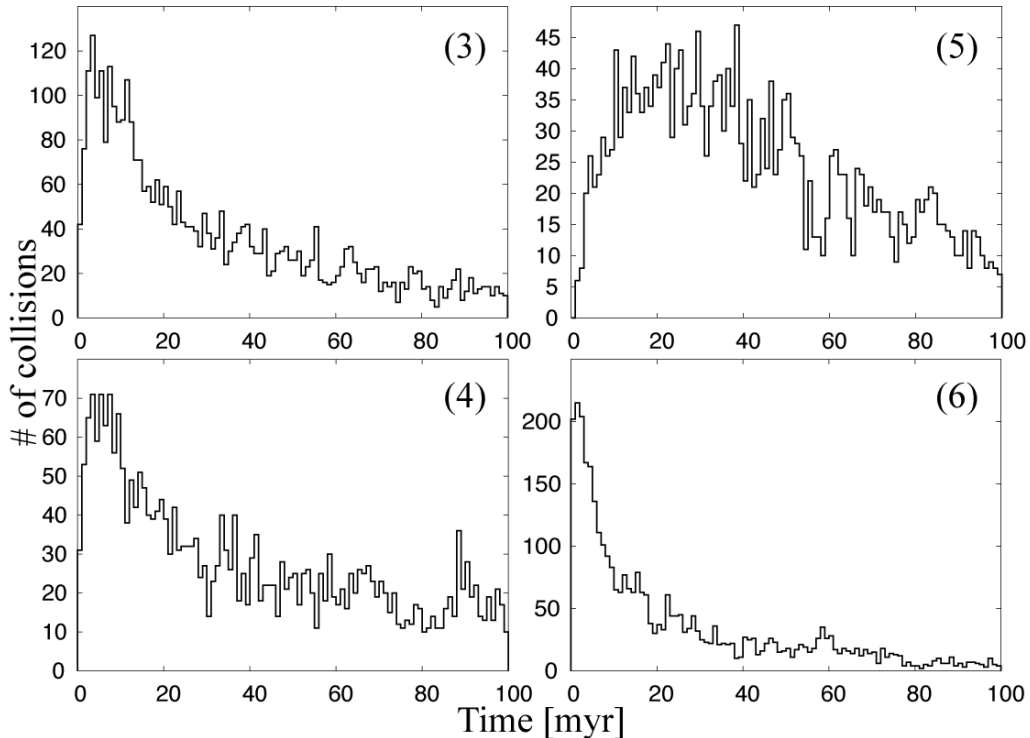


Fig. 4. Examples of the asteroid impact flux on the Moon when we used the initial condition sets (3)(4)(5) and (6).

leading/trailing asymmetry evident in Fig 3.) This can be used for comparison with the geographical data of the lunar crater distribution which exhibits global asymmetries (Morota and Furumoto, 2003, 2005). Detailed comparison will appear in future publications.

5 Summary and Conclusions

We have explored the dynamical evolution of test particles with initial conditions near the ν_6 resonance in order to simulate the orbital evolution of fragments from hypothetical asteroid break-up events. Compared with previ-

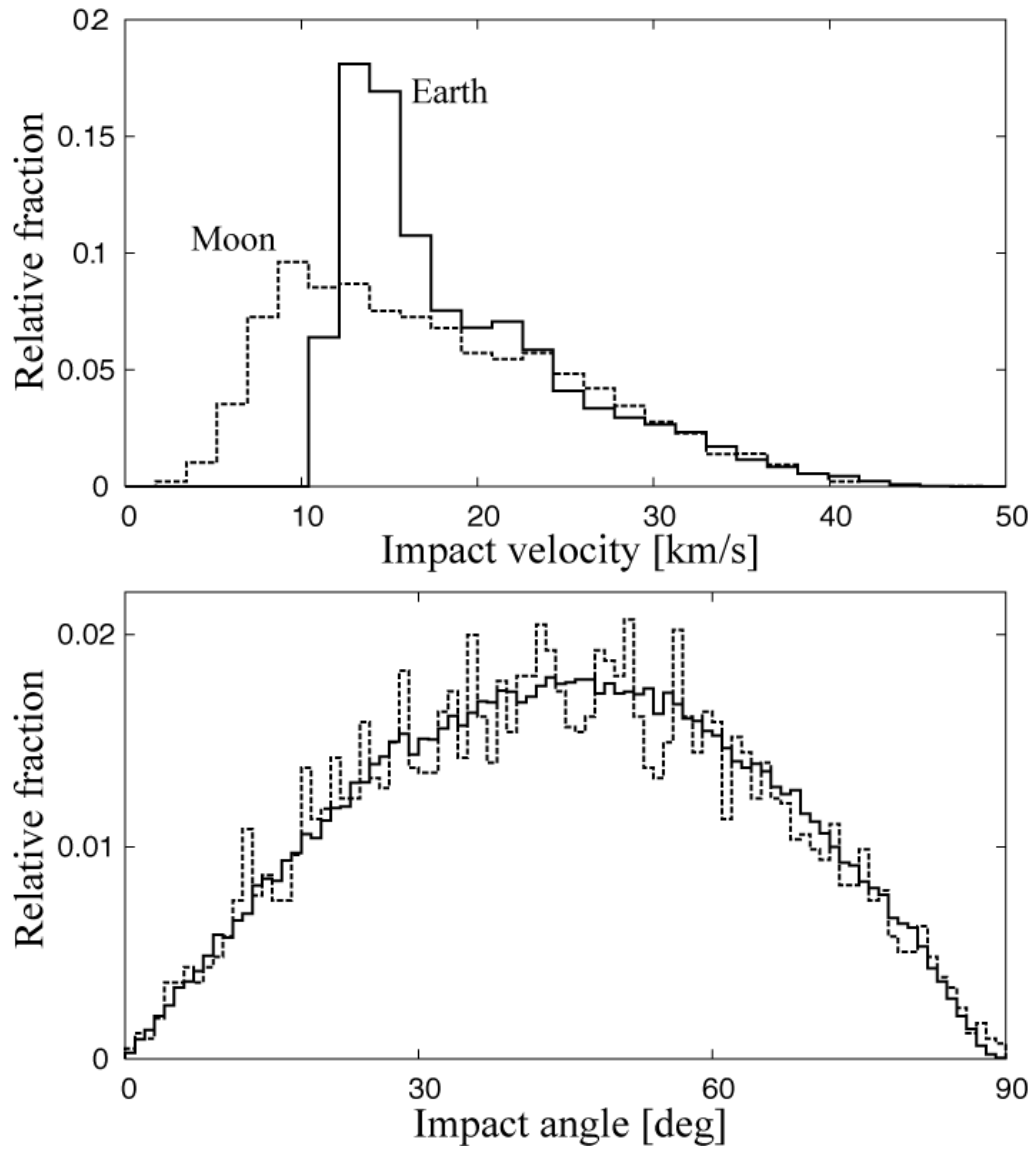


Fig. 5. An example of the distribution of the impact velocity (the upper panel) and angle (the lower panel) of clones in the case (2). In the lower panel, the solid line is for the Earth, and the dashed line is for the Moon.

ous studies such as Gladman et al. (1997) or Morbidelli and Gladman (1998), our simulations follow nearly two orders of magnitude larger number of particles. We calculated the collision probabilities on each of the terrestrial planets and on the Sun, and the dynamical lifetimes of asteroid fragments. Our improved statistics shows that the collision probability of asteroid fragments on the Earth is about 3% and on Venus is about 4–6%, not strongly sensitive to initial conditions in the vicinity of the ν_6 resonance in the low inclination part of the inner asteroid belt (Table 1). These numbers are slightly different from the numerical results presented in Gladman et al. (1997) that had yielded the collision probability of test particles from the ν_6 region on the Earth as 5.5% and that on Venus as 1.8%.

We also performed a set of orbital simulations of billions of cloned asteroid fragments inside of Earth’s activity sphere, including the dynamical motion of the Moon using the orbital distribution function of the particles calculated by the long-term orbital integration described above. From these simulations, we have obtained the collision probability, impact velocity, impact positions and impact angles of asteroid fragments on the Moon. These will be useful in a future study to compare with the observed lunar crater record. So far our simulations have only tested the particle dynamics with the current lunar orbit. But at 4 Ga the Moon could have been closer to the Earth (cf. Touma and Wisdom, 1994). The higher lunar orbital velocity and the greater gravitational focusing effect due to the lunar proximity to the Earth could both produce a dynamical effect on the collision probability of asteroids. Models of lunar evolution suggest that the Moon would experience a large increase in its orbital semimajor axis very early in its history and then gradually move away from the Earth over its remaining history; the distance and orbital velocity of the Moon with respect to Earth at the time of the LHB depend upon model parameters (tidal dissipation functions). This problem will be explored in a future study, as it might help to test models of lunar evolution.

Regarding the collision probability of the asteroid fragments on the Moon, we obtained a small value, $\sim 0.1\%$. The total mass of the LHB impactors on the Moon is estimated as $\sim 0.01\%$ lunar mass (Hartmann et al., 2000). Hence, if we ascribe LHB to a single asteroid disruption in the vicinity of the ν_6 resonance, we would need a very large parent body, as large as 1000–1500 km in diameter. (Moreover, the parent body would be required to be very close to the ν_6 resonance and to disrupt while it was in this short-lived orbit). This size should be considered a lower limit, because the collision probabilities would generally be lower for asteroid fragments from initial orbits of higher inclination or further from the ν_6 or from weaker resonances than the initial condition sets that we have simulated. Considering the fact that in the present main belt there is no asteroid larger than 1000 km diameter, the required size might seem rather improbable. We might need to consider the possibility that two or more asteroid disruptions happened at the time of LHB. Another ar-

gument against the likelihood of the large asteroid breakup hypothesis was recently presented Strom et al. (2005) that showed that the LHB crater size distribution is quite consistent with the size distribution of asteroidal projectiles from the main asteroid belt. The main belt asteroids have a complex and distinct size distribution (e.g. Jedicke and Metcalfe, 1998; Ivezić et al., 2001; Yoshida et al., 2003) probably as a result of a collisional cascade (Cheng, 2004; Bottke et al., 2005), and it is quite different from what would be expected for the fragments in a single collisional disruption (e.g. Michel et al., 2004). Both arguments above suggest that we should reject the large-asteroid-disruption hypothesis as a mechanism for the LHB.

The more likely cause of LHB may lie in the sweeping of strong resonances through the asteroid belt due to the orbital migration of giant planets (Levison et al., 2001; Gomes et al., 2005). In such a mechanism, the ν_6 secular resonance would be amongst the most powerful for causing asteroids to be excited into terrestrial planet-crossing orbits. The results presented here on the dynamics of asteroid impactors emerging from the vicinity of the ν_6 could be useful for the further study of this possible mechanism of the LHB. We note that in the present paper we have investigated only the dynamical effects of a stationary resonance, not a migrating resonance. Collision probabilities and impact velocities of asteroids might be different, depending on whether the resonance region is fixed (stationary) or migrating (sweeping). This is because in the vicinity of a resonance, there is a large range of timescales for the excitation of eccentricity, and there are differing amounts of phase space volume with the short versus long timescales. The short timescale zone enhances particle eccentricities quickly, so the impact velocity of an asteroid (with the planets and the Moon) will be higher, but the impact probability will be smaller. On the other hand, long timescale zone around a resonance is a source of asteroids that hit the planets with smaller impact velocity but with a higher probability because the gravitational focusing is more effective at lower velocity encounters. When resonances migrate due to planetary migration, the relative importance of the short timescale and the long timescale resonance zones would depend upon the speed of planetary migration. Future modeling of this mechanism is needed, especially the comparison of collision probabilities and impact velocities of asteroids of these two cases. It would also be important to obtain improved direct estimates the time duration of the LHB because it is directly related to the speed of resonance migration. For this purpose, more accurate chronology of lunar impact craters would help to constrain the dynamical mechanisms. This requires further lunar exploration, including sample-return missions.

Acknowledgements

The authors are grateful to the two referees of this paper, Alessandro Morbidelli and Bill Bottke, whose suggestions substantially improved the quality of the manuscript. This study is supported by the Grant-in-Aid of the Ministry of Education of Japan (16740259/2004–2005) and by NASA research grants NNG05GI97G (NASA-Origins of Solar Systems Research Program) and NNG05GH44G (NASA-Outer Planets Research Program).

References

- Bottke, W.F., Vokrouhlický, D., Brož, M., Nesvorný, D., and Morbidelli, A. Dynamical spreading of asteroid families by the Yarkovsky effect. *Science* 294, 1693–1696, 2001.
- Bottke, W.F., Durda, D.D., Nesvorný, D., Jedicke, R., Morbidelli, A., Vokrouhlický, D., and Levison, H.F. The fossilized size distribution of the main asteroid belt. *Icarus* 175, 111–140, 2005.
- Cellino, A., Michel, P., Tanga, P., and Zappalà, V. The velocity and implications for the physics of catastrophic collisions. *Icarus* 141, 79–95, 1999.
- Cheng, A.F. Collisional evolution of the asteroid belt. *Icarus* 169, 357–372, 2004.
- Cohen, B.A., Swindle, T.D., and Kring, D.A. Support for the lunar cataclysm hypothesis from lunar meteorite impact melt ages. *Science* 290, 1754–1756, 2000.
- Danby, J.M.A. *Fundamentals of Celestial Mechanics*. Willmann-Bell Inc., Richmond, Virginia, 1992.
- Gladman, B., Migliorini, F., Morbidelli, A., Zappalà, V., Michel, P., Cellino, A., Froeschlé, C., Levison, H.F., Bailey, M., and Duncan, M. Dynamical lifetimes of objects injected into asteroid belt resonances. *Science* 277, 197–201, 1997.
- Gladman, B., Michel, P., and Froeschlé, Ch. The near-Earth object population. *Icarus* 146, 176–189, 2000.
- Gomes, R., Levison, H.F., Tsiganis, K., and Morbidelli, A. Origin of the cataclysmic late heavy bombardment period of the terrestrial planets. *Nature* 435, 466–469, 2005.
- Farinella, P., Vokrouhlický, D., and Hartmann, W.K. Meteorite delivery via Yarkovsky orbital drift. *Icarus* 132, 378–387, 1998.
- Hartmann, W.K., Ryder, G., Dones, L., and Grinspoon, D. The time-dependent intense bombardment of the primordial Earth/Moon system. In: Canup, R. and Righter, K. (Eds.), *Origin of the Earth and Moon*, The University of Arizona Press, Tucson, Arizona, pp. 493–512, 2000.
- Ivezić, Ž., Tabachnik, S., Rafikov, R., Lupton, R.H., Quinn, T., Hammer-

- gren, M., Eyer, L., Chu, J., Armstrong, J.C., Fan, X., Finlator, K., Geballe, T.R., Gunn, J.E., Hennessy, G.S., Knapp, G.R., Leggett, S.K., Munn, J.A., Pier, J.R., Rockosi, C.M., Schneider, D.P., Strauss, M.A., Yanny, B., Brinkmann, J., Csabai, I., Hindsley, R.B., Kent, S., Lamb, D.Q., Margon, B., McKay, T.A., Smith, J.A., Waddel, P., and York, D.G. Solar system objects observed in the Sloan Digital Sky Survey commissioning data. *Astron. J.* 122, 2749–2784, 2001.
- Jedicke, R. and Metcalfe, T.S. The orbital and absolute magnitude distributions of main belt asteroids. *Icarus* 131, 245–260, 1998.
- Kring, D.A. and Cohen, B.A. Cataclysmic bombardment throughout the inner solar system 3.9–4.0 Ga. *Geophys. Res.* 107, E2, 4–1–4–6, 2002.
- Levison, H.F. and Duncan, M.J. The long-term dynamical behavior of short-period comets. *Icarus* 108, 18–36, 1994.
- Levison, H.F., Dones, L., and Duncan, M.J. The origin of Halley-type comets: probing the inner Oort cloud. *Astron. J.* 121, 2253–2267, 2001.
- Michel, P. and Thomas, F. The Kozai resonance for near-Earth asteroids with semimajor axis smaller than 2 AU. *Astron. Astrophys.* 307, 310–318, 1996.
- Michel, P., Benz, W., and Richardson, D.C. Catastrophic disruption of pre-shattered parent bodies. *Icarus* 168, 420–432, 2004.
- Morbidelli, A. and Gladman, B. Orbital and temporal distribution of meteorites originating in the asteroid belt. *Meteor. Planet Sci.* 33, 999–1016, 1998.
- Morbidelli, A. and Henrard, J. Secular resonances in the asteroid belts: theoretical perturbation approach and the problem of their location. *Celes. Mech. Dyn. Astron.* 51, 131–167, 1991.
- Morbidelli, A. and Nesvorný, D. Numerous weak resonances drive asteroids toward terrestrial planets orbits. *Icarus* 139, 295–308, 1999.
- Morota, T. and Furumoto, M. Asymmetrical distribution of rayed craters on the Moon. *Earth Planet. Sci. Lett.* 206, 315–223, 2003.
- Morota, T., T. Ukai and Furumoto, M. Influence of the asymmetrical cratering rate on the lunar cratering chronology. *Icarus* 173, 322–324, 2005.
- Ryder, G. Lunar samples, lunar accretion and the early bombardment of the Moon. *Eos* 71, 10, 313, 322–395, 1990.
- Strom, R.G., Malhotra, R., Ito, T., Yoshida, F., and Kring, D.A. The origin of impacting objects in the inner solar system. *Science* 309, 1847–1850, 2005.
- Tera, F., Papanastassiou, D.A., and Wasserburg, G.J.. A lunar cataclysm at ~ 3.95 AE and the structure of the lunar crust. *Lunar Planet. Sci. Conf.* 4, 723, 1973.
- Tera, F., Papanastassiou, D.A., and Wasserburg, G.J.. Isotopic evidence for a terminal lunar cataclysm. *Earth Planet. Sci. Lett.* 22, 1, 1974.
- Touma, J. and Wisdom, J. Evolution of the Earth–Moon system. *Astron. J.* 108, 1943–1951, 1994.
- Yoshida, F., Nakamura, T., Watanabe, J., Kinoshita, D., Yamamoto, N., and Fuse, T. Size and Spatial Distributions of Sub-km Main-Belt Asteroids. *Publ. Astron. Soc. Japan* 55, 701–715, 2003.

- Zahnle, K.J. and Sleep, N.H. Impacts and the early evolution of life. In: Thomas, P.J., Chyba, C.F., and McKay, C.P. (Eds.), *Comets and the Origin and Evolution of Life*, Springer-Verlag, New York, 175–208, 1997.
- Zappalà, V., Cellino, A., Dell'oro, A., Migliorini, F., and Paolicchi, P. Reconstructing the original ejection velocity fields of asteroid families. *Icarus* 124, 156–180, 1996.
- Zappalà, V., Cellino, A., Gladman, B., Manley, S., and Migliorini, F. Asteroid showers on Earth after family breakup events. *Icarus* 134, 176–179, 1998.